

<https://doi.org/10.15407/ujpe69.11.847>

P. JUCHA,¹ M. KLUSEK-GAWENDA,¹ A. SZCZUREK^{1,2}

¹ Institute of Nuclear Physics PAN

(Ul. Radzikowskiego, 152, PL-31342 Kraków, Poland;

e-mails: Pawel.Jucha@ifj.edu.pl, Mariola.Klusek@ifj.edu.pl)

² College of Natural Sciences, Institute of Physics, University of Rzeszów

(Ul. Pigońia, 1, PL-35-310 Rzeszów, Poland; e-mail: Antoni.Szczurek@ifj.edu.pl)

THE FUTURE OF EXPERIMENTAL MEASUREMENTS OF LIGHT-BY-LIGHT SCATTERING¹

Light-by-light scattering is a relatively new area in experimental physics. Our recent, theoretical research shows that studying two photon measurements in regions with lower transverse momentum ($p_{t,\gamma}$) and invariant mass ($M_{\gamma\gamma}$) allows us to observe not only the main contribution of photon scattering, known as fermionic loops, but also mechanisms like the VDM–Regge. In addition, examining diphoton measurements in low invariant mass regions is crucial for re-searching light meson resonances in $\gamma\gamma \rightarrow \gamma\gamma$ scattering. We also focus on the interference between different contributions. For future experiments with the ALICE FoCal and ALICE 3 detectors, we have calculated background estimates and explored possibilities to minimize their impact.

Keywords: heavy-ion collisions, ultraperipheral collisions, light-by-light scattering.

1. Introduction

Light-by-light scattering, a quantum electrodynamic process where two photons interact and scatter off each other, is a phenomenon observed for the first time at the Large Hadron Collider (LHC) in 2017 [1]. Light-by-light scattering can be observed due to the intense electromagnetic fields generated by the ultrarelativistic nuclei. These fields can be considered as a flux of quasi-real photons that surround the ions. When two ions pass by each other in ultraperipheral collisions, these electromagnetic fields can interact, enabling the light-by-light scattering.

Recent experiments at the LHC, conducted by the CMS [2] and ATLAS [3] collaborations, have successfully observed and measured light-by-light scattering in heavy ion collisions. However, both experiments use rather high thresholds for diphoton mass (5 GeV) and transverse momentum (2 GeV for CMS, and 2.5 GeV for ATLAS). The goal of our latest study [4] was to make predictions for future experiments with a

lower threshold for the mentioned parameters. Also, the study for different mechanisms, like VDM–Regge or light meson resonances, was conducted, searching for possibilities of their measurements.

2. Theoretical Formalism

The Equivalent Photon Approximation [5] relies on the knowledge about elementary cross section distribution in diphoton mass $W_{\gamma\gamma}$ and the scattering angle, $z = \cos \theta$. In this paper various mechanisms of $\gamma\gamma \rightarrow \gamma\gamma$ process are taken into consideration. The most common contribution is the four-vertex fermionic loops, so-called boxes, presented in Fig. 1, *a*. The calculation based on Feynman diagrams was carried out using FormCalc and LoopTools libraries based on *Mathematica* software [6]. To designate the cross sections for unpolarized photons, 16 photon helicity combinations of the amplitude must be added up. Due to symmetries, five contributions with correspondent weights were included:

$$\sum_{\lambda_1, \lambda_2, \lambda_3, \lambda_4} |\mathcal{A}_{\lambda_1 \lambda_2 \rightarrow \lambda_3 \lambda_4}^{\gamma\gamma \rightarrow \gamma\gamma}|^2 = 2 |\mathcal{A}_{++++}|^2 + 2 |\mathcal{A}_{+---}|^2 + 2 |\mathcal{A}_{+-+-}|^2 + 2 |\mathcal{A}_{+--+}|^2 + 8 |\mathcal{A}_{+--+}|^2. \quad (1)$$

Citation: Jucha P., Klusek-Gawenda M., Szczurek A. The future of experimental measurements of light-by-light scattering. *Ukr. J. Phys.* **69**, No. 11, 847 (2024). <https://doi.org/10.15407/ujpe69.11.847>.

© Publisher PH “Akademperiodyka” of the NAS of Ukraine, 2024. This is an open access article under the CC BY-NC-ND license (<https://creativecommons.org/licenses/by-nc-nd/4.0/>)

ISSN 2071-0194. *Ukr. J. Phys.* 2024. Vol. 69, No. 11

¹ This work is based on the results presented at the 2024 “New Trends in High-Energy and Low-x Physics” Conference.

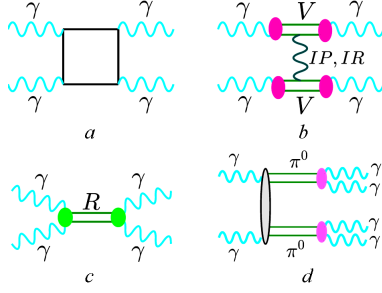


Fig. 1. Feynman diagrams of the LbL scattering mechanisms: fermionic loops (a), VDM-Regge (b), low-mass resonances in the s-channel (c), two- π^0 background (d)

The second mechanism of light-by-light scattering is double-photon hadronic fluctuation (Fig. 1, b). The mathematical description of the VDM-Regge mechanisms was studied in [7]:

$$\begin{aligned} \mathcal{M} = & \sum_{i,j} C_i^2 C_j^2 \left(C_{\mathbf{IP}} \left(\frac{s}{s_0} \right)^{\alpha_{\mathbf{IP}}(t)-1} F(t) + \right. \\ & + C_{\mathbf{IR}} \left(\frac{s}{s_0} \right)^{\alpha_{\mathbf{IR}}(t)-1} F(t) \left. + \right. \\ & + \sum_{i,j} C_i^2 C_j^2 \left(C_{\mathbf{IP}} \left(\frac{s}{s_0} \right)^{\alpha_{\mathbf{IP}}(u)-1} F(u) + \right. \\ & + C_{\mathbf{IR}} \left(\frac{s}{s_0} \right)^{\alpha_{\mathbf{IR}}(u)-1} F(u) \left. \right). \end{aligned} \quad (2)$$

The light meson resonances (Fig. 1, c) such as π , η and η' in $\gamma\gamma \rightarrow \gamma\gamma$ scattering is described based on relativistic Breit-Wigner formula presented in [8]:

$$\begin{aligned} \mathcal{M}_{\gamma\gamma \rightarrow R \rightarrow \gamma\gamma}(\lambda_1, \lambda_2) = \\ = \frac{\sqrt{64\pi^2 W_{\gamma\gamma}^2 \Gamma_R^2 B r^2 (R \rightarrow \gamma\gamma)}}{\hat{s} - m_R^2 - im_R \Gamma_R} \frac{1}{\sqrt{2\pi}} \delta_{\lambda_1 - \lambda_2}. \end{aligned} \quad (3)$$

In case of two photon measurement, the production of four photons from $\pi^0\pi^0$ decay (Fig. 1, d) where only two photons are observed in detectors constitutes the main background. However, based on description from [9], the idea how to reduce the background is discussed below.

The description of nuclear cross section for light-by-light is possible with the help of the Weizsäcker-Williams formula:

$$\frac{d\sigma(PbPb \rightarrow PbPb\gamma\gamma)}{dy_{\gamma_1} dy_{\gamma_2} dp_{t,\gamma}} =$$

$$\begin{aligned} = \int \frac{d\sigma_{\gamma\gamma \rightarrow \gamma\gamma}(W_{\gamma\gamma})}{dz} N(\omega_1, b_1) N(\omega_2, b_2) S_{abs}^2(b) \times \\ \times d^2 b d\bar{b}_x d\bar{b}_y \frac{W_{\gamma\gamma}}{2} \frac{dW_{\gamma\gamma} dY_{\gamma\gamma}}{dy_{\gamma_1} dy_{\gamma_2} dp_{t,\gamma}} dz. \end{aligned} \quad (4)$$

Here, the $\sigma_{\gamma\gamma \rightarrow \gamma\gamma}(W_{\gamma\gamma})$ is elementary cross section, $Y_{\gamma\gamma}$ is rapidity of outgoing two photons and \bar{b}_x , \bar{b}_y are the components of the vector $(\mathbf{b}_1 + \mathbf{b}_2)/2$, where $\mathbf{b} = \mathbf{b}_1 - \mathbf{b}_2$. The $N(\omega_i, b_i)$ is photon flux, which is obtained from charge distribution in the nucleus. The $S^2(b)$ denotes the survival factor. In recent studies, the sharp edge of nucleus ($S_{abs}^2(b) = \Theta(b - b_{max})$) was replaced by the formula:

$$S_{abs}^2(b) = \exp(-\sigma_{NN} T_{AA}(b)), \quad (5)$$

where σ_{NN} is the nucleon-nucleon interaction cross section, and $T_{AA}(b)$ is related to the so-called nuclear thickness function [4].

3. Elementary Cross Section Results

Calculation of the elementary cross section for light-by-light scattering show, that in diphoton invariant mass region below 1 GeV, one can expect significant signal from the loop contribution. Fig. 2, a displays the contributions of different fermions in the loop to this continuum. In Fig. 2, b the ratio of different contribution to the total cross section is presented. Here, the importance of interference is illustrated. The incoherent sum between quarkish and leptonic loops cannot sum up to 1. The impact of interference may be estimated to be around 20%.

The analysis of interference between different mechanisms was also conducted. In Fig. 3 the plot of ratios between the sum of two contributions (VDM-Regge, boxes) and clear box signal was shown as a function of $z = \cos\theta$ variable. The role of interference is clearly visible for the $|z| \rightarrow 1$. The smaller the scattering angle, the greater is the impact of VDM-Regge on the cross section. It is important to note that the effect of interference is destructive.

4. Nuclear Cross Section Results

The approach with smooth survival factor (Eq. (5)) was implemented to calculation of ATLAS data description. In Fig. 4, a the distribution of diphoton invariant mass for ATLAS kinematical cuts with sharp edge of nucleus and the survival factor based on

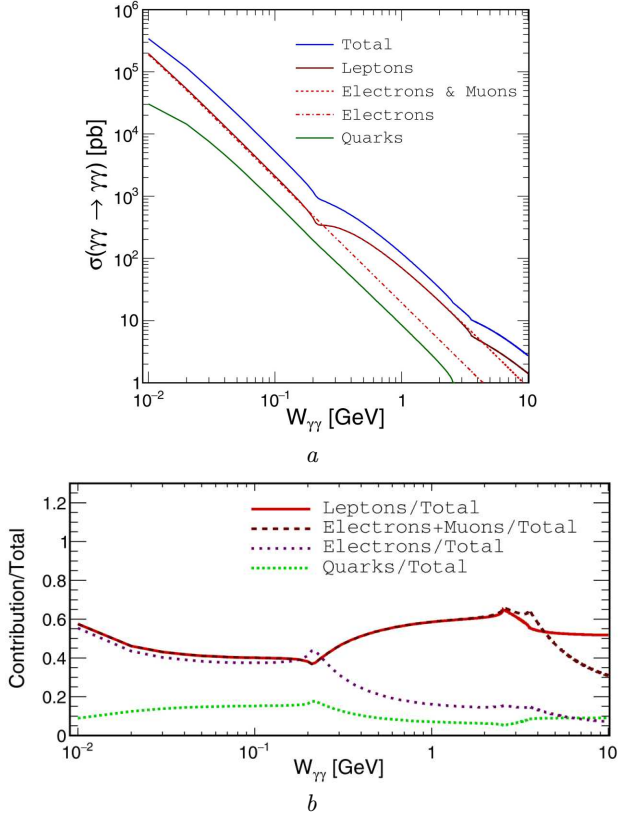


Fig. 2. Elementary cross section (in pb) as a function of energy. The total cross section (blue solid line) is split somewhat artificially into quarks (green solid line), electrons (red dashed line), electrons and muons (red dotted line), and leptons (red solid line) contributions (a); Ratio of each contribution to a coherent sum of them: leptonic cross section divided by total cross section (red solid line), quarks (green dotted line), electrons (magenta dash-dotted line) and sum of electron and muon contributions (dashed dark-red line) (b)

Eq. (5) is presented. All theoretical approaches, including SuperChic, underestimate the cross section in low-mass region. In Fig. 4, *b*, ratio between both our approaches for impact parameter cutoff is demonstrated. The difference is changing between 4% for smaller values of diphoton mass up to 10% for higher masses.

Planned forward detector for ALICE experiment – FoCal, will start collecting data since the Run 4 [11]. Kinematical cuts for photons were applied, to take advantage of the lower threshold for diphoton invariant mass ($M_{\gamma\gamma} > 500$ MeV), and the accessibility of larger photon rapidity ($3.4 < y_{\gamma_{1/2}} < 5.8$). The distribution of diphoton mass is presented in

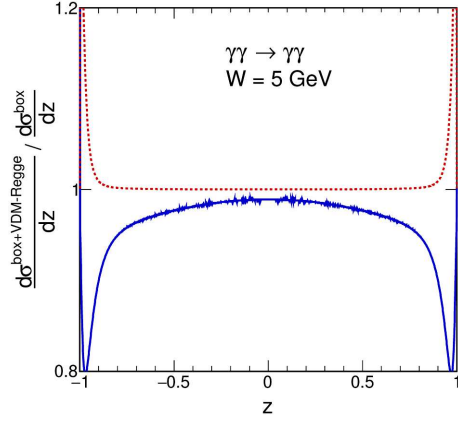


Fig. 3. The ratio of the coherent (blue, solid) and incoherent (red, dotted) sum of the box and VDM–Regge contributions divided by the cross section for the box contribution alone for $W = 5$ GeV

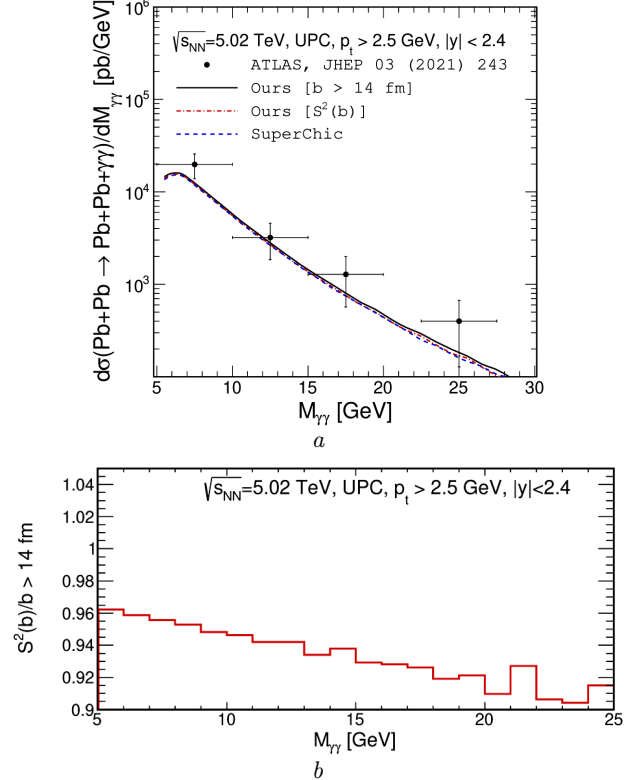


Fig. 4. Differential cross section as a function of the diphoton invariant mass at $\sqrt{s_{NN}} = 5.02$ TeV. The ATLAS experimental data are collected with theoretical results including a sharp cut on impact parameter ($b > 14$ fm – solid black line) and smooth nuclear absorption factor $S^2(b)$ (dash-dotted red line). Results obtained from SuperChic [10] is also shown for comparison (a). The ratio of the results calculated within our approach with sharp and smooth cut-off on impact parameter (b)

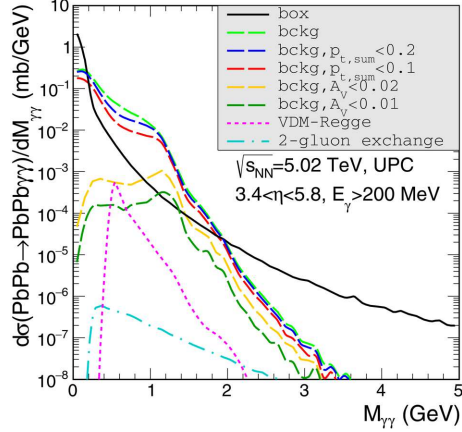


Fig. 5. Invariant mass distribution for the nuclear process – predictions for the future FoCal acceptance $E_{t,\gamma} > 200$ MeV and $3.4 < y_{\gamma_{1/2}} < 5.8$

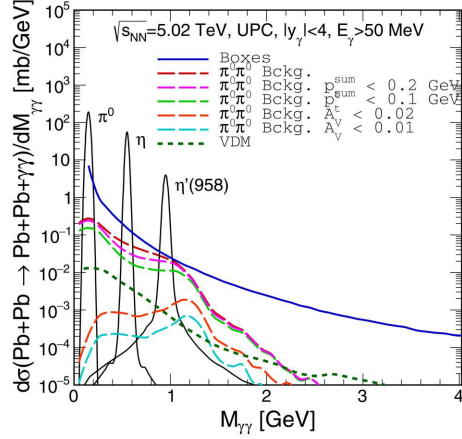


Fig. 6. Diphoton invariant mass distribution for ALICE 3, i.e., rapidity $y_{\gamma_{1/2}} \in (-4, 4)$ and photon energy $E_\gamma > 50$ MeV. Here, the black solid line represents the light meson resonances, the blue solid line relates to the box contribution, the dotted line to the VDM–Regge component and the dashed lines are for double- π^0 background contribution

Fig. 5. In this low-mass region, the background from the $\pi^0\pi^0$ production become significant. However, using isotropic distribution of photons in each π^0 decay, one can adjust the additional kinematical cuts to suppress the background. Hence, the cut for vector asymmetry $A_V = |\mathbf{p}_{t,1} - \mathbf{p}_{t,2}|/|\mathbf{p}_{t,1} + \mathbf{p}_{t,2}|$ was proposed. Implied cut notably reduce the measured cross section of $\pi^0\pi^0$ production.

From theoretical perspective, ALICE 3 experiment presents further opportunities for observation of light-by-light scattering. The calculation of cross sections

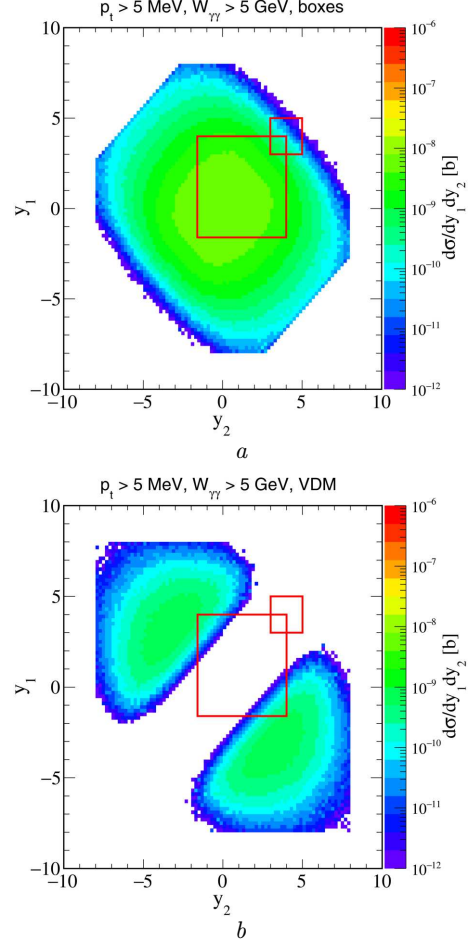


Fig. 7. Distribution in $(y_{\gamma_1}, y_{\gamma_2})$ in b for transverse momentum $p_{t,\gamma} > 5$ MeV, di-photon invariant mass $M_{\gamma\gamma} > 5$ GeV. Boxes (a), VDM–Regge mechanism (b)

were prepared based on the characteristic of the detector including kinematical limitations [12]. Fig. 6 shows the diphoton mass distribution in the assumed kinematical range. In the diphoton mass region below 1 GeV the most significant signal come from the mesonic resonances. The peaks from π^0 , η and η' overachieve even the box contribution, which will allow to observe this contribution for the first time. Here, the impact of the background also can be reduced using cuts on vector asymmetry.

The most challenging achievement would be a measurement of the VDM–Regge mechanism. Presented in Fig. 3 cross section distribution shows that the scattered photons in the VDM–Regge process are mainly forward/backward. This fact implies that the

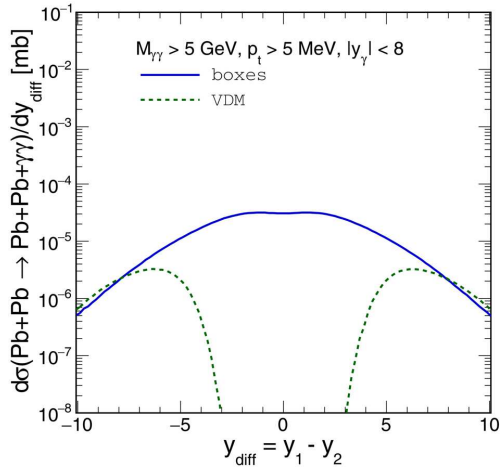


Fig. 8. Distribution in y_{diff} for light-by-light scattering processes in $\text{PbPb} \rightarrow \text{PbPb}\gamma\gamma$. Here, the transverse momentum cut is equal to 5 MeV. The blue solid line relates to the boxes, and the green dotted line to the VDM–Regge contribution. Here, the range of measured diphoton invariant mass is > 5 GeV

dedicated experiment has to have a broad range of photon rapidities. Fig. 7 presents a two-dimensional rapidity distribution of a) box continuum, b) VDM–Regge mechanism. The red squares represent the cover of rapidity ranges of the ALICE 3 barrel ($-1.6 < y_{\gamma_{1/2}} < 4$) and forward ($3 < y_{\gamma_{1/2}} < 5$) detectors. This plot reveals that current and planned experiments avoid region of interest.

However, the introduction of a new variable – the rapidity difference, may facilitate this observation. Figure 8 displays the distribution of the fermionic loops and the VDM–Regge mechanism in mentioned variable. For the higher values of $|y_{\text{diff}}|$ the chances for observing the VDM–Regge mechanisms increase.

5. Conclusion

The future development of new photons detectors opens up new opportunities for light-by-light scattering measurements. The lower threshold of diphoton mass clearly enable observation of light mesonic resonances. In recent studies, also the method of reduction of background from $\pi^0\pi^0$ was discussed. The final goal of future experimental measurements should be the observation of the VDM–Regge mechanism. However, required range of measured photon rapidity is difficult to achieved. Also, the extinguishing character of the interference between the

fermionic loops and the VDM–Regge mechanism generates additional difficulties.

Paweł Jucha would like to thank the organizers, in particular Prof. László L. Jenkovszky and Prof. Christophe Royon, for financial support, which enabled him to participate in the conference.

1. M. Aaboud *et al.* (ATLAS Collaboration). Evidence for light-by-light scattering in heavy-ion collisions with the ATLAS detector at the LHC. *Nature Phys.* **13** (9), 852 (2017).
2. A.M. Sirunyan *et al.* (CMS Collaboration). Evidence for light-by-light scattering and searches for axion-like particles in ultraperipheral PbPb collisions at $\sqrt{s_{NN}} = 5.02$ TeV. *Phys. Lett. B* **797**, 134826 (2019).
3. G. Aad *et al.* (ATLAS Collaboration). Observation of light-by-light scattering in ultraperipheral Pb+Pb collisions with the ATLAS detector. *Phys. Rev. Lett.* **123**, 052001 (2019).
4. P. Jucha, M. Klusek-Gawenda, A. Szczurek. Light-by-light scattering in ultraperipheral collisions of heavy ions at two future detectors. *Phys. Rev. D* **109**, 014004 (2024).
5. F. Krauss, M. Greiner, G. Soff. Photon and gluon induced processes in relativistic heavy-ion collisions. *Prog. Part. Nucl. Phys.* **39**, 503 (1997).
6. T. Hahn, M. Pérez-Victoria. Automated one-loop calculations in four and D dimensions. *Comp. Phys. Commun.* **118**, (2–3), 153 (1999).
7. M. Klusek-Gawenda, P. Lebedowicz, A. Szczurek. Light-by-light scattering in ultraperipheral Pb–Pb collisions at energies available at the CERN Large Hadron Collider. *Phys. Rev. C* **93**, 044907 (2016).
8. M. Klusek-Gawenda, R. McNulty, R. Schicker, A. Szczurek. Open Access Light-by-light scattering in ultraperipheral heavy-ion collisions at low diphoton masses. *Phys. Rev. D* **99**, 093013 (2019).
9. M. Klusek-Gawenda, A. Szczurek. $\pi^+\pi^-$ and $\pi^0\pi^0$ pair production in photon-photon scattering and ultraperipheral ultrarelativistic heavy-ion collisions. *Phys. Rev. C* **87**, 054908 (2013).
10. L.A. Harland-Lang, M. Tasevsky, V.A. Khoze, M.G. Ryskin. A new approach to modelling elastic and inelastic photon-initiated production at the LHC: SuperChic 4. *Eur. Phys. J. C* **80** (10), 925 (2020).
11. C. Loizides, W. Riegler *et al.* (ALICE Collaboration). Letter of intent: A Forward Calorimeter (FoCal) in the ALICE experiment, CERN-LHCC-2020-009, LHCC-I-036 (2020).
12. L. Musa, W. Riegler (ALICE Collaboration). Letter of intent for ALICE 3: A next generation heavy-ion experiment at the LHC. arXiv:2211.02491 (2022).

Received 07.10.24

П. Юха, М. Клусек-Гавенда, А. Щурек

МАЙБУТНЄ ЕКСПЕРИМЕНТАЛЬНОГО
ВИМІРЮВАННЯ РОЗСІЮВАННЯ
СВІТЛА СВІТЛОМ

Розсіювання світла на світлі є відносно новою областю в експериментальній фізиці. Наше нещодавнє теоретичне дослідження показує, що вивчення двофотонних процесів у області менших поперечних імпульсів ($p_{t,\gamma}$) і незмінною масою ($M_{\gamma\gamma}$) дозволяє нам спостерігати не тільки основний внесок розсіювання фотонів, відомий як ферміонні петлі, але і такі механізми, як VDM–Редже. Крім того, дослідже-

ння двофотонних процесів у області малих мас має вирішальне значення для дослідження резонансів легких мезонів у процесі розсіювання $\gamma\gamma \rightarrow \gamma\gamma$. Ми також звертаємо увагу на інтерференцію між різними внесками. Для майбутніх експериментів із детекторами ALICE FoCal і ALICE 3, ми зробили числові оцінки фону та дослідили можливості мінімізації його впливу на результати вимірювань.

Ключові слова: зіткнення важких іонів, ультрапериферійні зіткнення, розсіювання світла на світлі.